

# Modelling of the work processes high-pressure pump of common rail diesel injection system

Katarzyna Botwinska<sup>1,a</sup>, Remigiusz Mruk<sup>2</sup> and Łukasz Krawiec<sup>3</sup>

<sup>1,2,3</sup> *Warsaw University Of Life Sciences, Faculty of Production Engineering, Department of Production Organization and Engineering, Nowoursynowska 164, Warsaw, Poland.*

**Abstract.** Common rail injection systems are becoming a more widely used solution in the fuel systems of modern diesel engines. The main component and the characteristic feature of the system is rail injection of the fuel under high pressure, which is passed to the injector and further to the combustion chamber. An important element in this process is the high-pressure pump, continuing adequate pressure in the rail injection system. Common rail (CR) systems are being modified in order to optimise their work and virtual simulations are a useful tool in order to analyze the correctness of operation of the system while varying the parameters and settings, without any negative impact on the real object. In one particular study, a computer simulation of the pump high-pressure CR system was made in MatLab environment, based on the actual dimensions of the object – a one-cylinder diesel engine, the Farymann Diesel 18W. The resulting model consists of two parts – the first is responsible for simulating the operation of the high-pressure pump, and the second responsible for simulation of the remaining elements of the CR system. The results of this simulation produced waveforms of the following parameters: fluid flow from the manifold to the injector [ $\text{m}^3/\text{s}$ ], liquid flow from the manifold to the atmosphere [ $\text{m}^3/\text{s}$ ], and manifold pressure [Pa]. The simulation results allow for a positive verification of the model and the resulting system could become a useful element of simulation of the entire position and control algorithm.

## 1 Introduction

Nowadays, diesel engines are becoming more and more popular; modern diesel drives combine both driving dynamics and economy, which for many vehicle users is a key advantage. It is also the dominant power unit in the heavy vehicles sector, vehicle fleets, and machinery and equipment. It is also possible to achieve stricter emission reduction targets in terms of CO<sub>2</sub> into the air [1] with these engines. To optimise the operation of these engines and their emissions requires constant modifications and design improvements. Experimenting with real objects is usually very costly, time-consuming, and can result in damage or total destruction of the object. Therefore, nowadays computer simulations of the work of individual components as well as whole appliances are becoming increasingly popular. This allows you to estimate the functioning of the device at the given parameters without the risk of damage, enabling you to choose the best working configuration and implement it directly into the system, omitting the options that do not meet the requirements or expectations [2]. Because of the adjustable parameters of the injection system, and the resulting higher efficiency, power output, and lower noise and emission of the engine, CR injection systems are more commonly found in diesel engines. Their structure is based on the injection common rail - a rail wherein fuel is supplied by high-pressure pump from

a fuel tank. The pump provides the appropriate parameters of fuel pressure, which travels to the injectors via the rail and further to the combustion chamber. The injection rail keeps the fuel pressure constant until the injection. Due to the high operating pressure, together with a short injector opening time (milliseconds), the whole structure requires enormous precision and proper control. The cost of experiments on such sensitive systems is high, limiting the possibility of system failure [2,3].

The present study used simulation models to analyze the work of the high-pressure pump as an important component of the CR system, which provided the operating parameters of the system and is a useful tool in the process of designing and planning new systems.

### 1.1 The aims of the study

The aims of the study were:

1. To create a simulation of the processes occurring in the working fluid in a high pressure system in an engine with the common rail fuel system, based on a test stand to study the combustion process at the Department of Production Engineering at Warsaw University of Life Sciences (made and used by development project no. R10 037 03 Topic: "Application rapeseed crude oil as a fuel for diesel engines of tractors and agricultural vehicles");

<sup>a</sup> Corresponding author: katarzyna\_botwinska@sggw.pl

2. To create a simulation which will be useful as software for a control as well as collecting research data to study the combustion process.

### 1.2 Scope of the study

The scope of the study included:

- Description of the overall construction of the Common Rail with special attention to the conditions of liquid flow in the elements of the fuel feed pump, high-pressure lines, and manifold and the processes of mechanical work elements;
- The mathematical description of the flow of liquid through the above-indicated part of the high pressure system;
- The construction of the simulation model (simulation is not in real time) and analysis of the work of selected parts of the high pressure system and correct operation of control algorithms.

## 2 Materials & Methods

The simulation model was made in the Matlab Simulink environment. To build the model, the parameters of the real object - Farymann Diesel 18 W engine – were used. This is a single cylinder, four-stroke diesel engine used most often as drive for simple machines, e.g. Power generators and pumps. Below is a real object with the main elements:

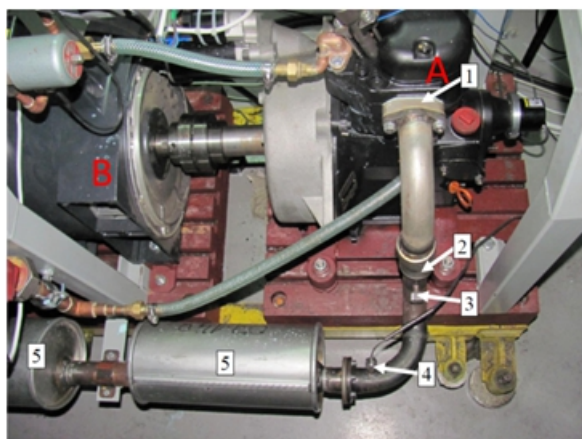


**Figure 1.** View of the engine - the real object with the main elements [(A) – Engine, (B) – Synchronous generator (brake), (1) – the exhaust pipe, (2) – bellows expansion joint, (3) – lock gas sampling (analyser chemical composition) (4) – sluice of thermocouple, (5) – silencers]

The key element for the simulation model part of the engine was the common rail injection system. Relevant for the simulation were:

- Common Rail system with Bosch CR / V4 / 10 -12S injector - a popular storage tank used in the CR systems of four-cylinder car engines. This rail allows connection of 4 injectors, however, due to the use of a single-cylinder, only one injector (also Bosch) was included;
- High-pressure pump Bosch model CR / CP1H3 – this provides the appropriate pressure up to a maximum of 150 [MPa]. Due to the reliability of the measurement results, the pump is supplied from an external source, controlled by an inverter.

The system with the main components is presented on Figure 2.

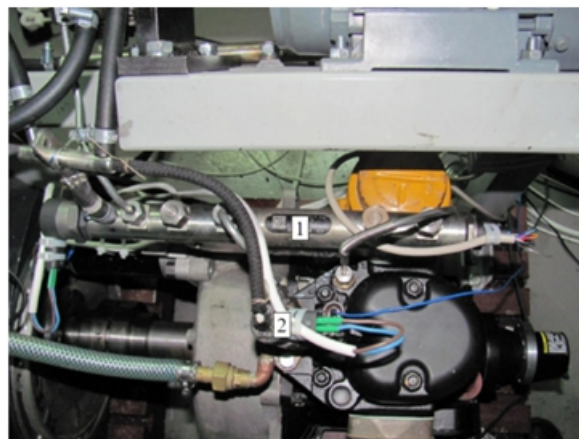


**Figure 2.** A view of Common Rail injection system in object [(1) – storage tank, (2) – CR injector electronically controlled].

The scheme of the high-pressure pump is presented in Figure 3.

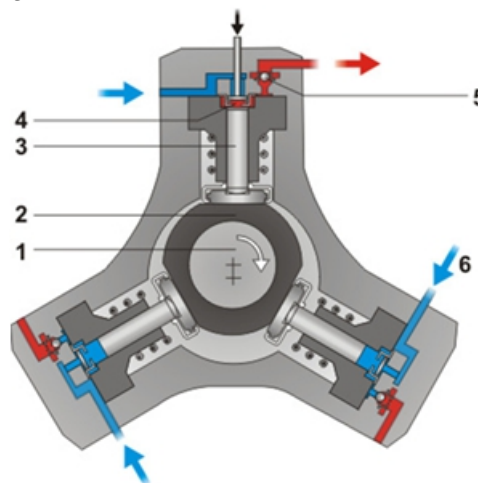


**Figure 3.** Diagram of the high pressure pump CP1 type [1] Drive shaft, 2) eccentric cam, 3) pressuring section, 4) inlet valve, 5) outlet valve, 6) fuel inlet, (source: <http://www.wtryskiwacz.com/jakie-mamy-pompy-wysokiego-cisnienia-Delphi-a-jakie-Bosch-naprawa-regeneracja.html>).

To build the model the following assumptions were adopted [4,5]:

- Fuel is a compressible liquid with elastic modulus  $E$  and is subject to the Hooke law;
- The elastic deformations of the injection pipe caused by changes in fuel pressure were ignored;
- The flow of fuel in the injection pipe is treated as a one-dimensional movement;
- The flow of fuel in the injection pipe is isothermal;
- The impact of friction is taken into account as are the movements of the elements of the injection system due to the effect of inertia, and damping forces of the springs and the fuel pressure of the system;
- Nominal pressure in the manifold is  $135 \cdot 10^6$  [Pa]
- Pump flow is equal to  $2 \cdot 10^{-2}$  [m<sup>3</sup>/s];
- The diameter of the high-pressure line is equal to  $2 \cdot 10^{-3}$  [m];
- The length of pipe from the pump to the collector is  $450 \cdot 10^{-3}$  [m];

- The length of pipe from the manifold to the channel inlet valve is  $1 \cdot 10^{-3}$  [m];
- The length of pipe from the collector to the injector is equal to  $300 \cdot 10^{-3}$  [m];
- The density of the fuel is constant and is equal to  $0,8247 = 0,8247 \cdot 10^3$  [kg/m<sup>3</sup>];
- Atmospheric pressure ( $p_{atm}$ ) is constant and is equal to  $1013,25 \cdot 10^2$  [Pa];
- Kinematic viscosity of diesel oil was assumed to be constant (independent of temperature) at  $3 \cdot 10^{-6}$  [m<sup>2</sup>/s];
- Radius of the ball on the valve head is equal to  $5 \cdot 10^{-3}$  [m];
- The mass of the valve head is equal to  $5 \cdot 10^{-3}$  [kg];
- The spring constant is equal to  $2500000$  [N/m];
- The volume of the manifold is equal to  $29 \cdot 10^{-6}$  [m<sup>3</sup>];
- The modulus of elasticity of the liquid ( $E_p$ ) are taken as a constant value independent of the temperature and equal to  $1441 \cdot 10^6$  [Pa].

Next, block diagrams [6,7,8,9,10] were constructed. To reflect the real operation of the system, a detailed model of the CR high-pressure pump was taken into account which consisted of parts listed below as Models to describe the movement of the piston pumping section. Below, the calculation diagram for the pumping section of the high-pressure CR pump is shown.

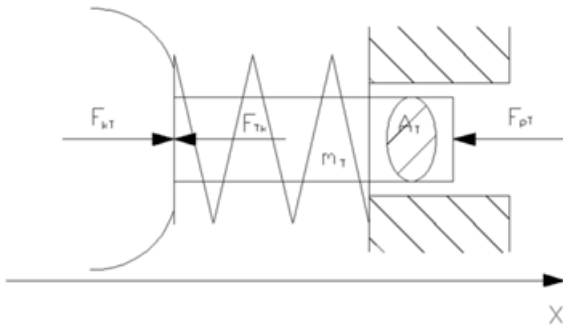


**Figure 4.** The calculation diagram of pumping section of the high pressure CR pump.

The movement of the piston pumping section was described by the mathematical model as follows:

$$X_k = (\cos \omega t)e + r \quad (1)$$

$$m_t \frac{d^2 x_t}{dt^2} = F_{kt} - F_{pt} - C \frac{dx_t}{dt} - F_{st} \quad (2)$$

$$F_{pt} = P_p A_t \quad (3)$$

$$F_{kt} = \begin{cases} 0: X_t - X_k \geq 0 \\ (X_t - X_k)K_t: X_t - X_k < 0 \end{cases} \quad (4)$$

where:

- $m_t$  – the mass of the piston,
- $F_{kt}$ – force on the piston from the cam,
- $F_{pt}$ –force of the fluid pressure,
- $F_{st}$ –spring force,
- $C$  – loss factors.

The force acting on the cam is calculated based on the instantaneous position of the piston and cam height with regard to the elasticity of the material. Then, using the Matlab Simulink environment, the simulation model was built to describe the movement of the piston pumping

section, which can be seen below.

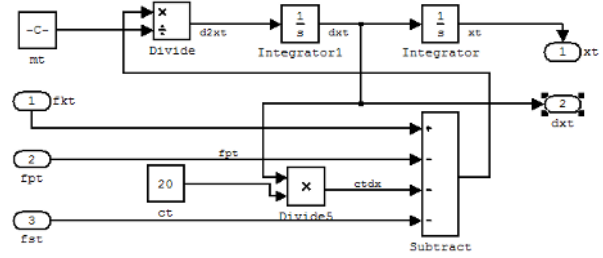


**Figure 5.** The simulation model to describe the movement of the piston pumping section.

Next, models of the high-pressure chamber of the CR pump were built. The calculation diagram for the high-pressure chamber of the CR pump which was used is shown below.

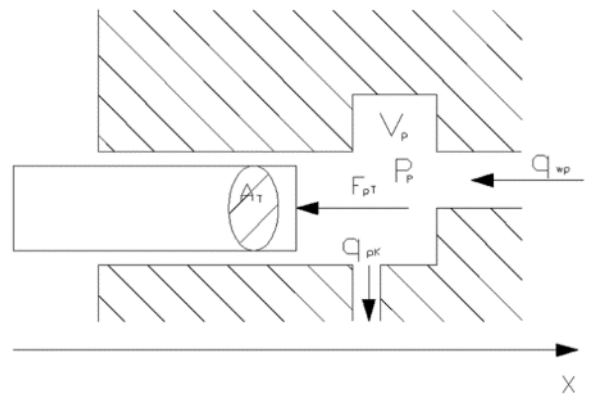


**Figure 6.** The calculation diagram of high pressure chamber of the CR pump.

The high-pressure chamber of the CR pump was described by the mathematical model as follows:

$$\frac{V_p dp_p}{E_p dt} = q_{wp} - q_{pk} + A_t \frac{dx_t}{dt} \quad (5)$$

where:

- $V_p$  – volume of the chamber,
- $p_p$ – chamber pressure,
- $q$ - liquid streams,
- $X_t$ - the position of the piston,
- $A_t$  – cross-sectional area of the piston.

Using the Matlab Simulink environment, the simulation model for the high-pressure chamber of the CR pump was built which can be seen below.

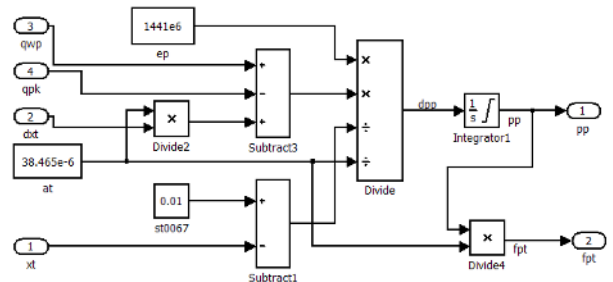


**Figure 7.** Simulation model of the high pressure chamber of the CR pump.

Another section was the mathematical model of the ball valve, the calculation diagram is shown below.

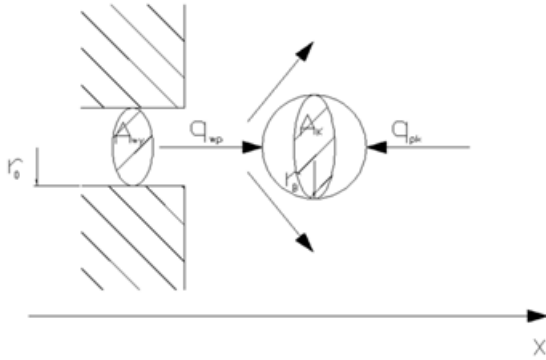


**Figure 8.** The calculation diagram of ball valve.

The ball valve was described by the mathematical model as follows:

$$m_k \frac{d^2 X_k}{dt^2} = F_{kwy} - F_{wek} + F_{0k1} - F_{0k2} - C \frac{dx_4}{dt} \quad (6)$$

$$F_{kwy} = A_{kul} P_{kom} \quad (7)$$

$$F_{wykul} = A_{kul} P_{wy} \quad (8)$$

$$F_{0kul1} = \begin{cases} 0: X_k \geq 0 \\ -K_k X_k: X_k < 0 \end{cases} \quad (9)$$

$$F_{0kul} = \begin{cases} 0: X_k + P_k \leq 5 \\ K_{kul}(X_k - P_k): X_k + P_k > 5 \end{cases} \quad (10)$$

where:

- $m_k$  – ball mass,
- F- forces acting on the ball,
- C- loss factor,
- $X_k$ - the position of the ball.

Then, using the Matlab Simulink environment, the simulation model of the ball valve was built, which can be seen in Figure 9.

Mathematical models of the plate valve were also built and the calculation diagram of the plate valve is shown in Figure 10.

The final part of this section is a comprehensive model of the high-pressure pump. Below, the complete mathematical model to describe the movement of the piston pumping section is shown.

$$m_z \frac{d^2 X_z}{dt^2} = F_{0zp1} - F_{0zp2} + F_{cpz} + F_{wez} - F_{pz} \quad (11)$$

$$F_c = -C_{pz} \frac{dx_{pz}}{dt} \quad (12)$$

$$F_{wezp} - F_{pzp} = (P_{we} - P_p) A_p \quad (13)$$

$$K_{0zp1} = \frac{E(A_{zp} - A_{we})}{I_{zp}} \quad (14)$$

$$F_{0p1} = \begin{cases} 0: X_{zp} \geq 0 \\ -K_{zp} X_{zp} - C_{0zp} \frac{dx_{zp}}{dt}: X_p < 0 \end{cases} \quad (15)$$

$$F_{0p2} \begin{cases} 0: X_p - 1 \leq 0 \\ X_p - 1 > 0: (X_p - 1) K_{0zp2} \end{cases} \quad (16)$$

$$q_{PK} = C_D \pi D_{pz} X_p \sqrt{\frac{2(P_{we} - P_{wy})}{\rho}} \text{sign}(p_{we} - p_{wy}) \quad (17)$$

where:

- $m_z$  – weight of the valve plate,
- F- forces acting on the plate,
- C- loss factor,
- $X_k$ - position of the plate.

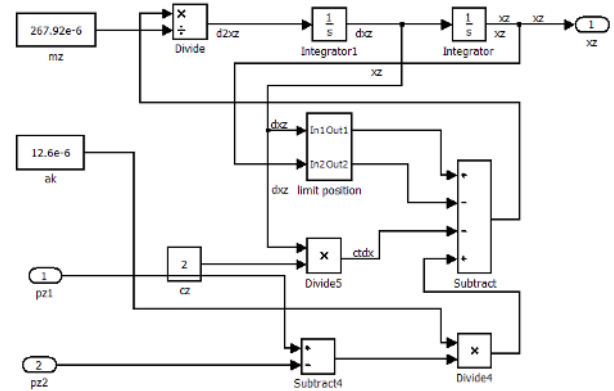


**Figure 9.** Simulation model of the ball valve.

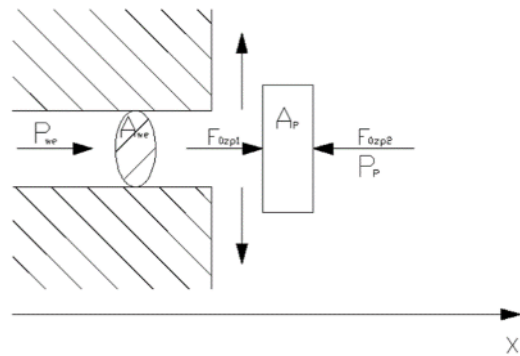


**Figure 10.** The calculation diagram of plate valve.

Another large section in providing the real operation of the system was construction of a simulation model for the other elements of the CR (simplified models). For this purpose, a calculation scheme is shown below.

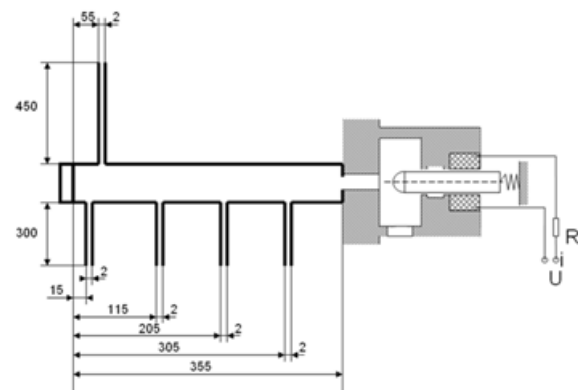


**Figure 11.** The calculation diagram of part of the high pressure CR system.

This section consisted of:

1. The equation of continuity in the manifold, as shown below:

$$0 = u_{zpomba} \cdot A_{zpomba} \cdot \sqrt{\frac{2}{\rho} \cdot p_{str}} - u_{zatm} \cdot A_{zatm} \cdot \sqrt{\frac{2}{\rho} \cdot p_z - p_{atm} - p_{str}} - u_{z1} \cdot A_{z1} \cdot \sqrt{\frac{2}{\rho} \cdot p_z - p_{atm} - p_{str}} - \frac{V_z}{E_p} \frac{dp_z}{dt} \quad (18)$$

where:

- A – surface for the identified cables,
  - $u_{zpompa}$  - flow loss factor between the pump and the manifold,
  - $p_z$  – pressure in accumulation pipe,
  - $p_{pompa}$  – pressure in the fuel supply channel to the chamber,
  - $p_{atm}$  – output pressure in control chamber,
  - $\mu$  - flow losses factor.
- and the part of simulation model responsible for liquid continuity equation in manifold.

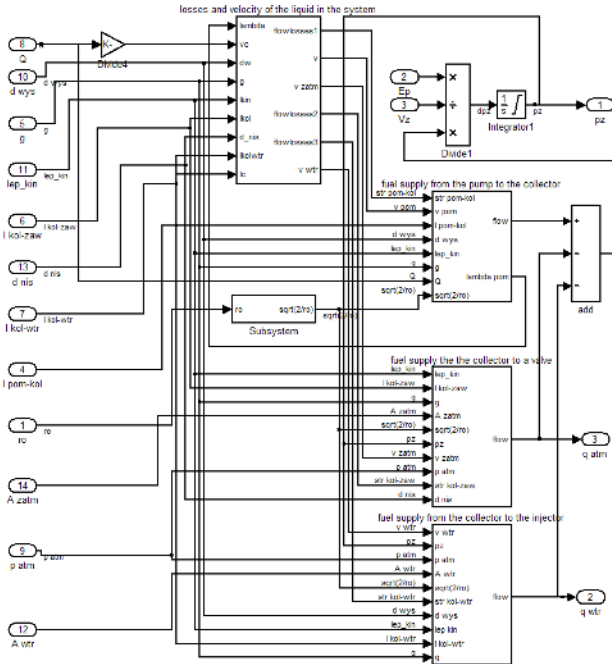


Figure 12. Scheme corresponding to liquid continuity equation in manifold.

2. The flow loss factor between the pump and the manifold. The hydraulic flow loss factor between the pump and the manifold is described by the equation (19) and modelled in Figure 13.

$$u_{zpompa} = \lambda \frac{l \cdot v^2}{d \cdot 2 \cdot g} + 0,5 \quad (19)$$

where:

- $\lambda$  – linear loss factor of turbulent flows,
- l – length of the pipe from the pump to the manifold,
- v – average velocity of fluid flow,
- d – the diameter of the cable leading from the pump into the manifold,
- g – acceleration of gravity.

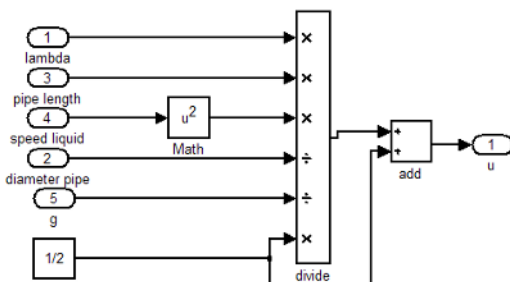


Figure 13. The flow loss factor.

3. The part of simulation model responsible for fuel supply to the injector.

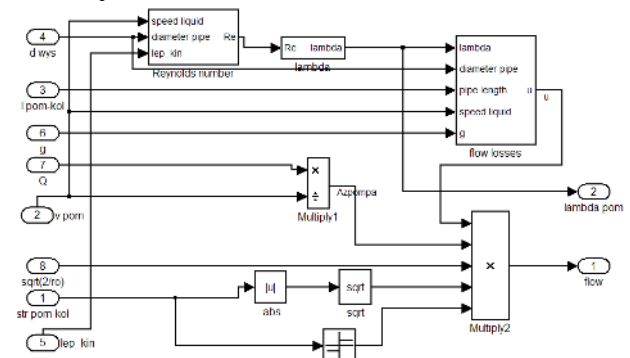


Figure 14. The model of fuel supply to the injector.

4. The mathematical equation in the model is the equation of valve head movement of the pressure regulating valve in the manifold.

$$m \frac{d^2w}{dt^2} = -u \frac{dw}{dt} - k \cdot w + B \cdot i \quad (20)$$

where:

- m – movable part mass,
  - v – kinematic viscosity factor,
  - w – displacement of the movable part,
  - k – spring constant,
  - B·i – force produced by the acting magnetic field on, current flowing through the coil.
5. The part of the model responsible for temporary opening of the valve, depending on the parameters prevailing in the system.

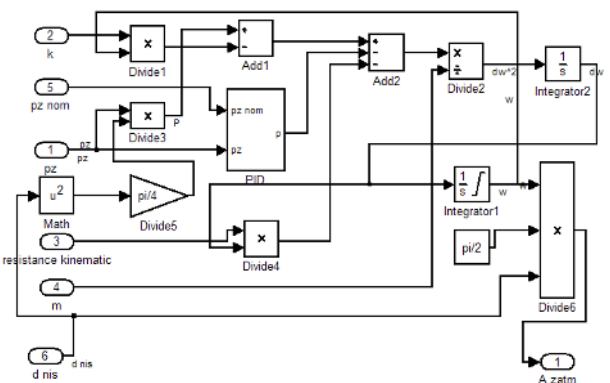


Figure 15. Model describing temporary opening the valve, depending on the parameters prevailing in the system.

6. The scheme for the PID regulator manifold pressure (moved to the control software) shown below.

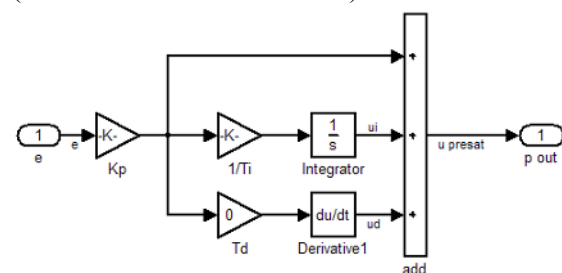


Figure 16. Simulation scheme of PID regulator manifold pressure (moved to the control software).

### 3 Results

Having finished the simulation model, a computer simulation for the given parameters was conducted. The following presents the results of simulations in terms of waveforms: liquid flow from the manifold to the injector [ $\text{m}^3/\text{s}$ ], liquid flow from the manifold to the atmosphere [ $\text{m}^3/\text{s}$ ], and pressure in the manifold [Pa] for set parameters and a period of time to 0.7 [s].

- The pressure waveforms in the manifold at a pressure of 100 mPa at a given time from 0 to 0,07 [s] (initial state) – Figure 17.

In the initial phase it can be seen that the fluid flow from the manifold to the injector takes the form of regular peaks every 0,01 [s], starts at 0 to 0,001 [ $\text{m}^3$ ]. The liquid flow from the collector to the atmosphere at the beginning changes rapidly in a range from 0,0013 to 0,0023 [ $\text{m}^3$ ], then over a period of 0,01 [s] reaches a value of about 0,003 [ $\text{m}^3$ ], then decreases to a value of 0,00255 [ $\text{m}^3$ ] and stabilizes. Manifold pressure in the initial phase (from 0 to 0,02 [s]) varies in the range from 0,00114 to 0,0096 [Pa], and then stabilizes in and around 0,001 [Pa].

- The pressure waveforms in the manifold at a pressure of 100 [MPa] and the opening of the injector (1%) over a period of 0,04 to 0,07 [s] (Figure 18).

During the opening of the injector (1%) in a range from 0,04 to 0,07 [s], a slight increase in the flow time of liquid from the manifold to the injector 0 - 0,001 [ $\text{m}^3$ ] can be observed. The liquid flow from the collector into the atmosphere during 0,01 [s] initially falls rapidly, then stabilizes, increases, and after that is recurrent in time intervals. Pressure in the manifold is more variable. In each interval (0,01 [s]), pressure initially drops sharply (the minimum value for a single pitch 0,0094 [Pa]) and then increases (the maximum value for a single stroke 0,01015 [Pa]) The pressure waveforms in manifold at a predetermined pressure of 100 [MPa] and the opening of the injector (5%) over a period of from 0,04 to 0,07 [s].

- The pressure waveforms in the manifold at a predetermined pressure of 100 [MPa] and the opening of the injector (5%) over a period of 0,04 to 0,07 (Figure 19).

During the opening of the injector (5%), elongation of fluid flow in time can be observed as well as increase of flows over 0,001 [ $\text{m}^3$ ]. For fluid flow from the manifold to the atmosphere, stabilizing in the value in the time interval of 0.01 [s] can be observed. The pressure in the manifold assumes a greater range of variation in comparison with the opening of the injector (1%).

- The pressure waveforms in the manifold at a predetermined pressure of 100 [MPa] and the opening of the injector (10%) over a period of 0,04 to 0,07 [s] (Figure 20).

During the opening of the injector (10%), further elongation of the liquid flow over time can be observed, together with an increase in the range of values for liquid flow from the manifold to the atmosphere from 0,00256 to 0,0028 [ $\text{m}^3$ ], and increase in the range of changes of pressure in the manifold.

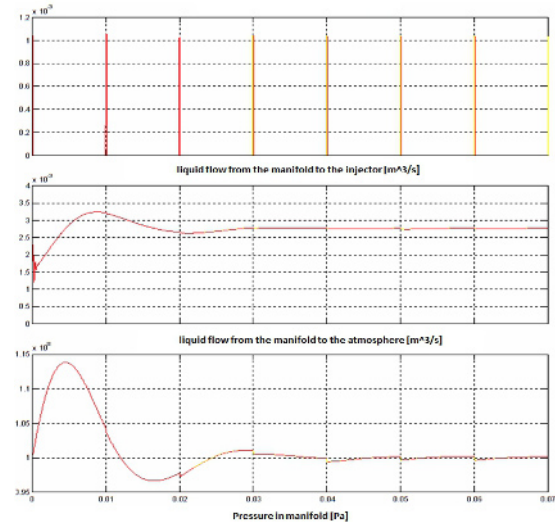


**Figure 17.** The pressure waveforms in the manifold at a pressure of 100 mPa at a given time from 0 to 0,07 [s] (initial state).

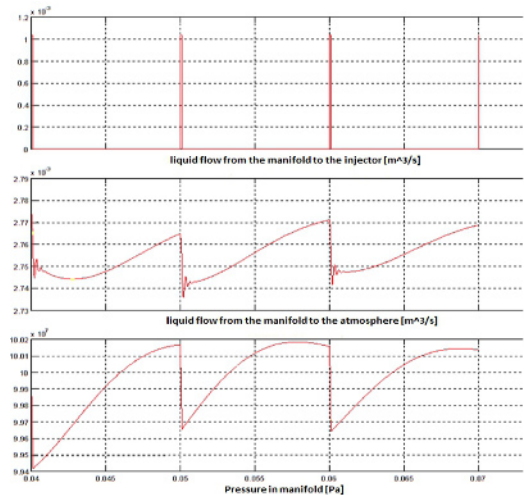


**Figure 18.** The pressure waveforms in the manifold at a pressure of 100 [MPa] and the opening of the injector (1%) over a period of 0,04 to 0,07 [s].

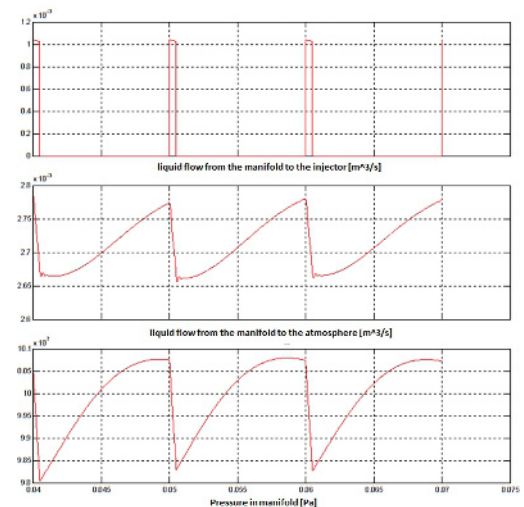


**Figure 19.** The pressure waveforms in the manifold at a predetermined pressure of 100 [MPa] and the opening of the injector (5%) over a period of 0,04 to 0,07 [s].

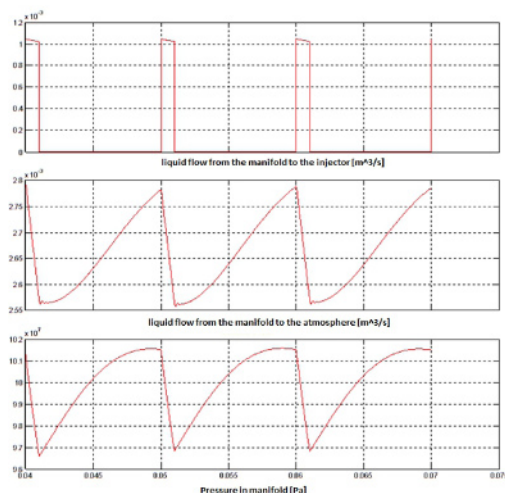


**Figure 20.** The pressure waveforms in the manifold at a predetermined pressure of 100 [MPa] and the opening of the injector (10%) over a period of 0,04 to 0,07 [s].

## 4 Conclusions

On the basis of the constructed model, simulations conducted, and the results obtained, the following conclusions can be made:

- The basic aim of this study was to build a dependence which automatically delineating change the manifold pressure in the common rail system during engine operation on the basis of certain parameters.
- The authors have shown and described the simulation model and then checked for correctness on the basis of simulations.
- The results of simulation allow for verification of correct construction of the structure diagrams - Full verification of the functionality of the model will be carried out on a real object in future studies.
- Correct results indicate that the high-pressure control system, built in the simulation, would operate in a stable manner.

## References

1. Press materials Robert Bosch GmbH, *The future of the diesel engine - will be electrified?*, <http://mojafirma.infor.pl/moto/wiadomosci/rynek/324193,Przyszlosc-silnika-Diesla-zostanie-zelektryfikowany.html>.
2. A. Szuliborski, *Controlling compression ignition engines information Technical BOSCH* (Publishing Transport and Communications, Warsaw 2004)
3. H. Günther, *Common Rail injection systems in practice workshop: construction, testing, diagnostics* (Publisher of Communications and Communications, Warsaw 2010)
4. N.H. Chung, B. G. Oh, and M. H. Sunwoo, *Modelling and injection rate estimation of common-rail injectors for direct-injection diesel engines* (Journal of Automobile Engineering 222.6 (2008): 1089-1001)
5. C. Gautier, O. Sename, L. Dugard, G.Meissonnier, *Modelling Of A Diesel Engine*

*Common Rail Injection System* (IFAC 16th World Congress, Prague 2005)

6. B. Mrozek, Z. Mrozek, *Matlab Simulink 2.x 5.x User's Guide* (PLJ Publisher, Warsaw 1998)
7. T.A. Kumar, *MATLAB and Simulink for Engineers* (Oxford 2011)
8. D. Xue, Y.Q. Chen, *System Simulation Techniques with MATLAB and Simulink*, (Wiley Publisher, 2013)
9. M. Gołębiewski, M. Walkowski, *Common Rail systems in the combustion engines and selected phenomena occurring in the fuel pipes of high pressure during the fuel injection* (Scientific Journals 2009, 17(89) pp. 38–43)
10. T. Gancarczyk, T. Kniefel, *Modelling Analyses of Common Rail High Pressure Pump* (Mechanik, 2013, R. 86, nr 2CD.)